

# Venous Detectability with 9.4-T BOLD 3D Microscopy: Comparison with Two-photon Microscopy

S-H. Park<sup>1,2</sup>, K. Masamoto<sup>3</sup>, I. Kanno<sup>3</sup>, and S-G. Kim<sup>1,4</sup>

<sup>1</sup>Radiology, University of Pittsburgh, Pittsburgh, PA, United States, <sup>2</sup>Bioengineering, University of Pittsburgh, Pittsburgh, PA, United States, <sup>3</sup>Molecular Imaging Center, National Institute of Radiological Sciences, Inage, Chiba, Japan, <sup>4</sup>Neurobiology, University of Pittsburgh, Pittsburgh, PA, United States

## Introduction

High-resolution vascular imaging, capable of detecting small veins, will give investigators a tool to understand the relationship between BOLD fMRI signal and vascular structures. BOLD-based venography has shown detailed venous structures at high fields [1,2,3]. Since venous diameters are not directly measurable by BOLD, detectability of this technique has not been clearly demonstrated. In this study, venous density was quantified for data acquired by 9.4-T BOLD 3D microscopy, and the results were compared with diameter-dependent venous density measured by 3D two-photon laser scanning microscopy. The diameter of the smallest vessel detectable by our BOLD studies was then determined by density comparisons between the two imaging modalities.

## Materials and Methods

Eleven male Sprague-Dawley rats weighing 260–450 g were used for MRI studies ( $N = 6$ ), and for two-photon microscopy studies ( $N = 5$ ). For all studies, the rats were mechanically ventilated under 1.2–1.5% isoflurane anesthesia in an air:O<sub>2</sub> mixture with FiO<sub>2</sub> = 30–35%. The femoral artery and femoral vein were catheterized for blood gas sampling and for fluid administration, respectively. Rectal temperature was maintained at  $37 \pm 0.5$  °C with a water-heating pad, controlled by a thermocouple and feedback unit.

MR experiments were carried out on a Varian 9.4 T / 31-cm MRI system with a 12-cm I.D. Magnex gradient coil. A home-built quadrature RF surface coil (I.D. of each of 2 lobes = 1.6 cm) was provided RF excitation and reception. Voxel-localized shimming was performed. BOLD microscopy was performed with a 3D flow-compensated gradient-echo pulse sequence. The RF power level was adjusted to maximize subcortical signal. Imaging parameters were: TR = 50 ms, TE = 20 ms, FOV =  $3.0 \times 1.5 \times 1.5$  cm<sup>3</sup>, matrix =  $384 \times 192 \times 192$ , and total scan time = 34 min 38 s. Bilateral rectangular columns perpendicular to the cortical surface within the 3D dataset were defined in the somatosensory cortex (1.0 mm posterior and  $\pm 2.6$  mm lateral to bregma) with a flattened cross-sectional area of  $1.8 \times 1.8$  mm<sup>2</sup> and a length spanning the entire cortical depth (59- $\mu$ m isotropic resolution). Veins were identified within each column for the regions with cortical depth  $\geq 0.4$  mm only if they passed criteria based on intensity threshold (85% of average tissue signal intensity, Fig. 1g) and depth contiguity (connected over at least 4 continuous planes). At cortical depths of 0.4, 1.0, and 1.6 mm, density was then quantified based on the venous size defined by number of in-plane contiguous pixels (small: 1–5, medium: 6–10, and large:  $\geq 11$ ) within a smaller  $1.4 \times 1.4 \times 0.059$  mm<sup>3</sup> region concentric with the  $1.8 \times 1.8 \times 0.059$  mm<sup>3</sup> region, to minimize problems associated with veins located at the edges of each plane.

For two-photon microscopy, the left parietal bone was thinned ( $5 \times 7$  mm<sup>2</sup>) and a 0.2–0.4 ml bolus of Qdot<sup>®</sup> 605 (1  $\mu$ M) was intravenously injected. Using the same coordinates as the MR studies, four images were acquired ( $0.456 \times 0.456$  mm<sup>2</sup>) for each cortical depth in 0.01-mm steps from the surface to 0.6 mm, and combined to make the ROI size larger ( $0.91 \times 0.91$  mm<sup>2</sup>). Veins were discriminated from other vasculature by tracking pial venous networks. Venous density and diameter were quantified at 0.1 and 0.4 mm depths.

## Results and Discussion

The distribution of veins as a function of cortical depth for one animal is illustrated in Fig. 1. Intracortical veins appear as small spots due to their perpendicular orientation in a flattened plane (Fig. 1b) defined along the middle of cortex (yellow line in Fig. 1a). Pial veins are observed in the plane near the cortical surface (Fig. 1c). Fewer intracortical veins are visualized with increased cortical depth (Fig. 1d–f). Figure 1g shows that a histogram of Fig. 1d deviates from a Gaussian fitting for intensity below  $\sim 85\%$  of the average tissue signal intensity. As cortical depth increases, the density of these identifiable veins decreases for “small” and “medium” veins (Friedman test,  $p < 0.05$ ), but not for “large” veins (Fig. 1h). This implies that smaller-diameter veins are more numerous in the shallow cortical regions, while larger-diameter veins drain the deeper regions of the cortex, in agreement with vascular anatomy [4]. The density of identifiable veins of all sizes was  $5.7 \pm 1.0$ ,  $3.5 \pm 1.0$ , and  $1.5 \pm 0.6$  / mm<sup>2</sup> (12 hemispheres) at cortical depths of 0.4, 1.0, and 1.6 mm, respectively.

In two-photon microscopy study, capillary networks in the 3D datasets were also traceable from the source where penetrating arterioles branched to the draining venules (Fig. 2a and b). Diameter-dependent intracortical venous density (Fig. 2c) shows high density of relatively small veins (5–30  $\mu$ m) with a sparse distribution of larger veins. When only veins with diameter  $> 10$ , 15, and 20  $\mu$ m are considered, venous density was  $11.1 \pm 3.9$ ,  $5.3 \pm 1.8$ , and  $3.4 \pm 1.6$  / mm<sup>2</sup>, respectively, at the cortical depth of 0.4 mm. The results imply that the diameter of the smallest vein detectable by 9.4-T BOLD microscopy under our conditions is  $\sim 15$   $\mu$ m.

## References

1. Ogawa et al, Magn Reson Med 16:9-18 (1990) 2. Christoforidis et al. J Comput Assist Tomogr 23:857-866 (1999). 3. Park et al, Proc Intl Soc Mag Reson Med 1718 (2005). 4. Nakai et al, Stroke 2:653-659 (1981).

Supported by NIH grants (NS44589, EB003324, EB003375)

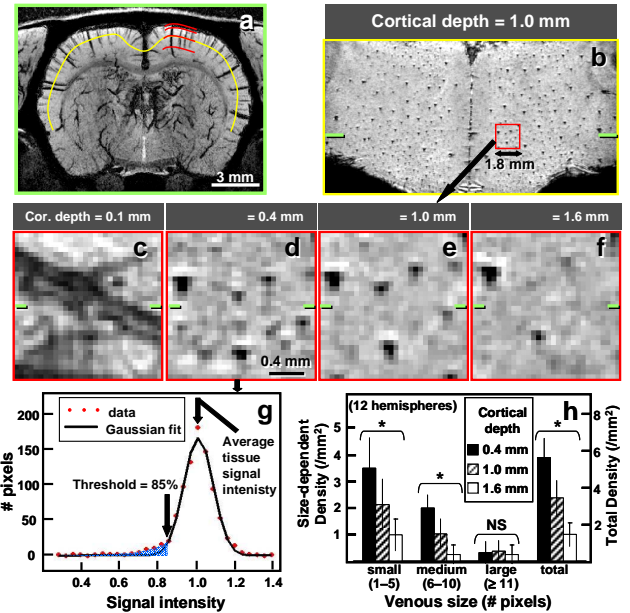


Figure 1. Reconstructions from a MR dataset and cortical depth-dependent venous quantification. **a**: Minimum-intensity projection of a 1-mm thick coronal slab. Red curves indicate cortical depths of 0.1, 0.4, 1.0, and 1.6 mm. **b**: A single-pixel thick (59- $\mu$ m) reconstruction at the location of the yellow curve in **a**. **c–f**: Expanded views of regions at (c) 0.1, (d) 0.4, (e) 1.0, and (f) 1.6 mm from the cortical surface. The green ticks in **b–f** represent the slab center of **a**. **g**: Histogram of **d** and its Gaussian curve fitting. Blue-colored region shows venous pixel candidates. **h**: Depth-dependent quantification of intracortical venous parameters for all studies ( $N = 6$ , 12 hemispheres). \*  $p < 0.05$ ; NS = no significant difference.

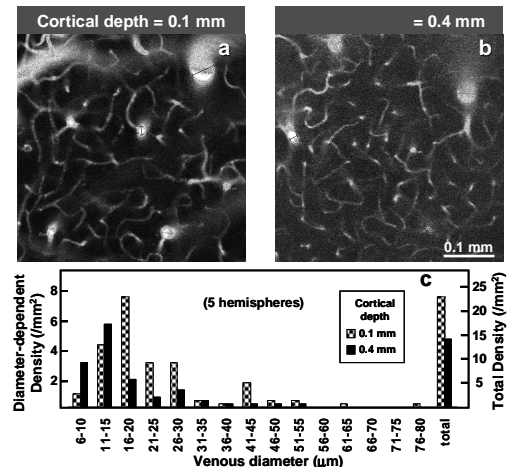


Figure 2. Reconstructions from 3D *in vivo* two-photon laser scanning microscopy datasets and cortical depth-dependent quantification of venous distributions. Ten images were maximum-intensity projected at cortical depths of 0.1 mm (**a**) and 0.4 mm (**b**). Venous densities are plotted as a function of cross-sectional diameter (**c**).